HYDROGEN BUBBLE DISPERSION AND SURFACE BURSTING BEHAVIOUR

Ingram, J.M.,[1] Battersby, P., Averill, A.F., Holborn, P.G. and Nolan, P.F.

Hydrogen Hazards Unit, London South Bank University (LSBU), London SE1 0AA. United Kingdom, [1]ingramja@lsbu.ac.uk

ABSTRACT

In many processes where hydrogen may be released from below a liquid surface, there has been concern regarding how such releases might ultimately disperse in an ullage space. Knowledge of the extent and persistence of any flammable volume formed is needed for hazardous area classification as well as for validation of explosion modelling or experiments. Following an initial release of hydrogen, the overall process can be subdivided into three stages (i) rise and possible break-up of a bubble in the liquid, (ii) formation and bursting of a thin gas-liquid-gas interface at the liquid surface and (iii) dispersion of the released gas. An apparatus based on a large glass sided water tank has been constructed which employs two synchronised high-speed imaging systems to record the behaviour of hydrogen bubble release and dispersion. A high-speed digital video system records the rising of the bubbles, and the formation and bursting of the gas-liquid-gas interface at the liquid surface. An additional schlieren system is used to visualise the hydrogen release as bubbles burst at the liquid surface. The bubble burst mechanism can clearly be described from the results obtained. Following the nucleation of a hole, surface tension causes the liquid film to peel back rapidly forming a ring/torus of liquid around the enlarging hole. This process lasts only a few milliseconds. Although some hydrogen can be seen to be expelled from the bubble much seems to remain in place as the film peels away. To assess the extent of the flammable plume following a bubble burst, the apparatus was modified to include an electric-arc igniter. In order to identify plumes coincident in space with the igniter, a schlieren system was built capable of recording simultaneously in two orthogonal directions. This confirmed that clouds undetected by the schlerien imaging could not be ignited with the electric arc igniter.

1.0 INTRODUCTION

In nuclear sites, hydrogen can be formed by radiolysis or corrosion as well as from dissolved hydrogen coming out of solution. Hydrogen releases can be in the form of bubbles from hold-up in sludge and those bubbles might vary from small, dispersed bubbles to large releases of several hundred litres. Another potential source of hydrogen might be from enclosed, pressurised volumes such as storage flasks, drums and pipe volumes.

It is important to know how these releases disperse. The extent and persistence of the flammable region needs to be assessed for hazardous zoning (DSEAR). Secondly, an understanding of the dispersion process strengthens the validity of modelling and the design of experiments to assess the consequences of an explosion following a release. Pessimistic assumptions regarding dispersion can lead to unrealistically high estimates of ignition probability, as more ignition sources are likely to be considered as coincident with a release (and vice versa). A particular area of concern is where hydrogen might be released as a bubble or stream of bubbles from beneath a liquid surface. Whilst attempts have been made to construct simple models to represent such releases for specific scenarios, these have had limited usefulness because of the lack of test data to validate them. Experimental results are required to allow the extent of the flammable region formed by a transient hydrogen release to be more accurately determined. It is necessary, not only to visualise the dispersion of hydrogen once a bubble has burst, but to track the rise of the bubble in the liquid and clearly see the manner in which bursting occurs at the surface. Because the visualisation of hydrogen using schlieren techniques measures concentration gradient rather than specific hydrogen concentration, it is difficult to

determine whether the flammable region extends beyond the visible schliere. Consequently, in order to relate the intensity of a visible schliere from a bursting bubble to concentration/flammability, an experimental programme involving deliberate ignition of bubble plumes at set distances from the water surface was also carried out.

2.0 EXPERIMENTAL

2.1. Bubble rise and dispersion experiments

A diagram of the experimental arrangement is shown in Figure 1. The apparatus consists of a large glass-sided water tank and two synchronised high-speed imaging systems: a standard high-speed digital imaging system and a second schlieren system.

The water tank is 0.8×0.8m in section and 1.5m tall. Two opposite sides of the tank were made from 19mm toughened glass so that when filled with water, the thickness is enough to keep bending of the panes to an extent (< 2mm) acceptable for standard video imaging. However, it was considered that schlieren images would be affected by stresses in the surface of the glass from the toughening process. For this reason, the tank was completely filled with water thus enabling schlieren imaging of bubbles bursting at the surface to be undertaken. The other sides of the tank are made from 8mm thick mild steel plate covered with an epoxy coating whilst the base, also made from 8 mm thick plate was covered with a 3mm neoprene sheet to avoid damage to the glass during construction. The four uprights extend above the liquid level so that sides/roof can be added above the water level if required to simulate a vessel ullage. Isolated bubbles of hydrogen of relatively small volume were produced in the experiments by slowly passing gas from a blending panel of rotameters through a U-shaped tube at the bottom of the tank. U tubes of different sizes between 3.3mm and 13mm internal diameter were used to generate bubbles in the region of 0.1 to 2.5 cm^3 in volume.

In order to visualise hydrogen releases, a general-purpose, 2-mirror, Z-type schlieren system [1] was set up using two high quality ($\lambda/10$), 0.20 m diameter, spherical mirrors of 1.8 m focal length. Illumination was provided by a light box, masked with a 1mm by 3mm slit and an Olympus i-Speed digital camera was used to record the images. A knife-edge with adjustable mount provided the optical cut-off necessary for the schlieren effect to be seen. The height of the optical components (as shown) is such that the bottom edge of the mirrors (whose diameter limits the field of view) is just below the level of the water/glass, allowing the bursting bubble to be seen.

The rise of bubble through the liquid and emergence at the surface was filmed using a Photron Fastcam-1024PCI 100K high-speed camera. It was necessary to position this slightly off-axis due to a combination of physical constraints and the thermal plume from the camera interfering with the schlieren imaging. The Photron camera was set up to send both an external trigger signal and frame speed signal to synchronise its frames with the Olympus i-speed images. Above the tank there is a retractable rod (an air-operated piston). This provides an object to focus the cameras on during set-up and allows the hydrogen outlet to be positioned so that the bubbles can be seen to break at the position of the rod.

The air-operated piston was activated to push the rod into shot. After the cameras were focused on the position of the rod, the hydrogen flow rate was set on a rotameter on the blending panel. This allowed a bubble to be released every few seconds. The position of the bubble release was adjusted so that the bubble broke the surface at the position of the rod. In this way, it was known that the bubbles would be in focus. Both cameras were set to record in continuous mode. This mode writes image data to the storage buffers until they are full, then overwrites the oldest images in sequence. As a bubble was seen to rise past a mark made on the tank, the piston control and the camera trigger were both pushed. Respectively, these caused the piston to retract the rod out of shot and triggered the cameras to record and stop. Images from the cameras were analysed using Olympus "De-luxe" i-Speed software.

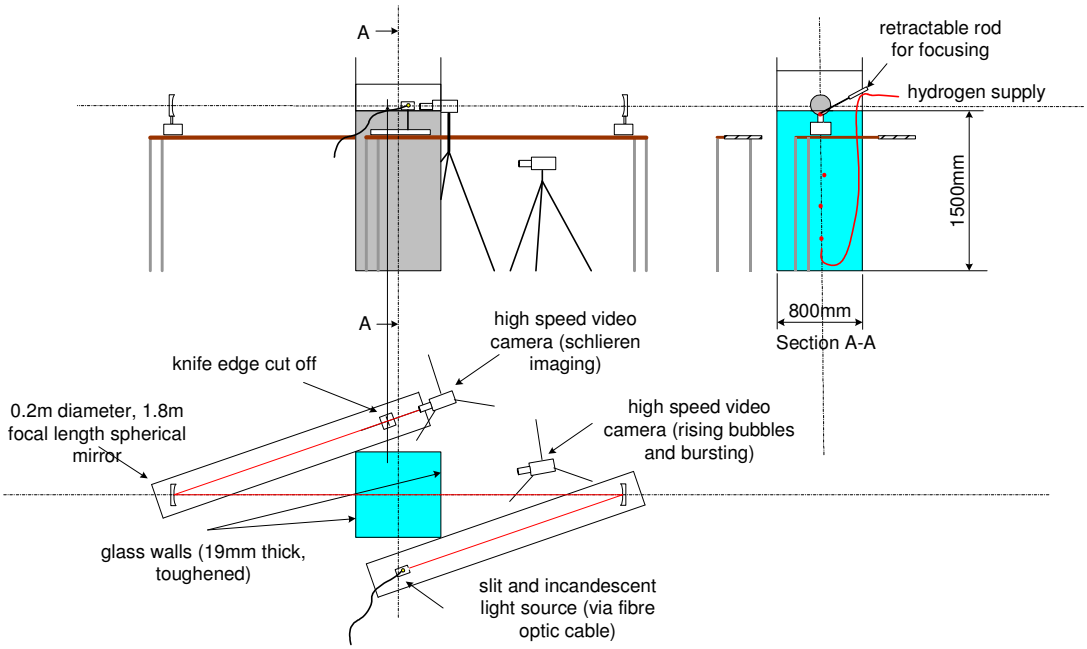

Figure 1. Diagram showing water tanks and imaging systems

The rod, visible in the early frames of the film, was used to calibrate the software so that measurements could be taken from the images. Bubbles were sized using images from the Photron camera. Smaller bubbles tended to be spherical and were easily sized whereas larger bubbles tended to distort, oscillating around a "cap" shape (segment of a sphere). In this case, images were selected when the bubble most closely approximated a spherical segment and measurements were taken from those images.

The digital images from the Olympus camera showed the bubble breaking the surface and the hydrogen dispersing. The images were used to estimate the distance from the epicentre of bursting to the furthest point at which the movement of hydrogen could not be seen on the schlieren images. This was recorded as the visible detection limit.

Visualisation of the schlieren images could be enhanced by digital post-processing using Adobe Photoshop software. An image from the video sequence just prior to the emergence of a bubble was used as a background image and then inverted (made a negative). An image of a later frame was then pasted as a layer over the inverted background image and the opacity of the layer set to 50%. This effectively subtracts the background from the image of interest yielding an almost uniformly grey image. Differences between the image being analysed and the background show up over a very narrow range of grey levels. These differences are the schlieren information that show the movement of hydrogen. The two image layers could then be merged. The human eye can only resolve around 20 grey levels whereas a digital image from the camera has 256. This means that the human eye can only see 20/256ths (about 1/13th) of the grey scale information on the bitmap image. However, as the schlieren information is distributed over a narrow range of grey levels (coincidentally about 20 grey scale levels on the bitmap) digital contrast stretching can be used to enhance the image. The grey levels are adjusted so that the narrow range of interest is rescaled over a wider range and becomes visible to the naked eye. Thus light grey becomes white and dark grey becomes black. Figure 2 shows a schlieren image before and after post-processing.

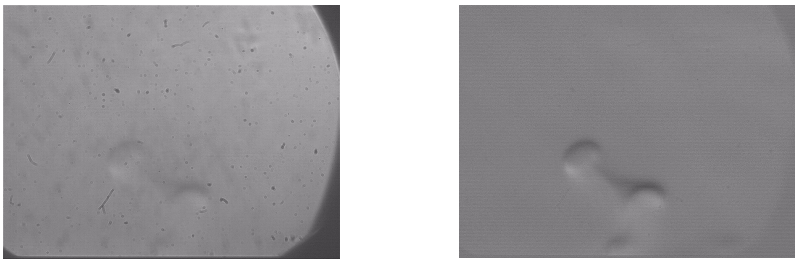

Figure 2 Example schlieren image before and after post-processing

2.2 Experimental determination of visible schliere flammability

This set of experiments was conducted as schlieren essentially measures a concentration gradient. It was therefore necessary to (i) confirm that the flammable region does not extend beyond the visible schliere and (ii) relate the intensity of the visible schliere from a bursting bubble to concentration/flammability. To accomplish this, a system of deliberate ignition of bubble plumes at set distances from the water surface was employed.

The apparatus, i.e. tank and bubble release mechanism, was in most respects similar to that described above for the bubble dispersion experiments. It was configured to produce bubbles of around 20mm diameter. The ignition source employed, based on a 10 kV, 20 mA ignition transformer, was capable of providing a continuous arc for short periods of time (~30 s, Figure 3). A series of tests was conducted to verify the igniters ability to ignite near flammable limit mixtures. For these tests, premixed hydrogen/air was supplied through a 52 mm internal diameter pipe, to provide a low velocity flammable plume just under the igniter. Near the flammable limit it became unclear if the mixtures were burning or if the schliere present on the image were due to refractive index gradients caused by heat from the electric arc. The approach was modified by orienting the electrodes horizontally and placing a thin plastic shield near the electrode tips. The shield restricted the hot air from the arcing to one side of the image, so any schliere present on the other side of the image could be attributed to combustion of hydrogen-air mixtures. Using this arrangement, it proved possible to visualise combustion of hydrogen-air mixtures down to 6.25% (v/v) hydrogen in air. Below this concentration, it was not possible to visualise any combustion.

The igniter electrodes were bolted to a metal frame, such that they could be suspended different distances above the water surface. Because of the difficulty in determining whether or not any particular two-dimensional schliere that appears to touch the igniter has in fact done so, it was necessary to add a second schlieren system. The orthogonal arrangement, shown in Figure 4, comprised a single standard Z system with two extra plane mirrors set up in the field of view to allow the igniter to be viewed.

For the schliere ignitability tests, three different igniter heights were investigated; 40, 53 & 65mm. The maximum height was still significantly below the height above the surface at which the schliere becomes undetectable. All the tests were performed with the release of 17 mm diameter (2.5 cm^3) bubbles. The hydrogen flow rate was adjusted so that individual bubbles would have time to burst on the surface and fully disperse before the arrival of the next bubble. Next, the igniter was turned on and the high speed camera triggered. After 30s the igniter and recording was stopped. The digital images were then reviewed to identify which plumes missed one or both orthogonal images. For bursts where it was recognised that the plume touched the electrodes in both images, it was noted whether or not ignition had occurred. Repeating this process enabled ignition frequencies to be determined for each of the three igniter heights

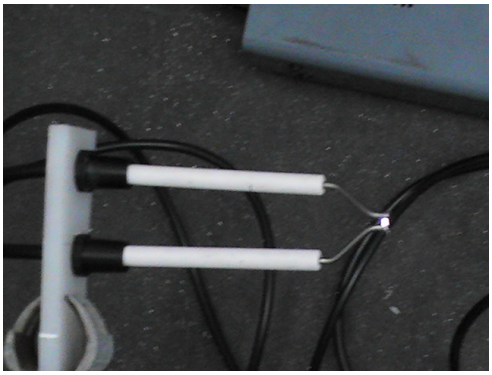

Figure 3. Close-up of the igniter's electrodes. Arcing can be seen

2.3. Imaging hydrogen bubble bursting behaviour

The apparatus and general procedure involved in the experiments to examine the nature of bubble bursting at the surface of the liquid in more detail were essentially the same as described above. However, in contrast to the earlier work the second high speed camera was also focused on the water/ air interface to capture normal video images of the bubble burst at high frame rate (6000 fps). The positioning of the camera itself was the same as in the earlier work, i.e. slightly off-axis due to a combination of physical constraints and the thermal plume from the camera interfering with the schlieren imaging. Additional lighting was necessary and this was supplied by two Portaflash DL1000 Digi Lights positioned one either side of the tank at roughly 90 degrees to the glass sides. Both schlieren and normal video images were then analysed using the Olympus i-Speed software. The rod, visible in the early frames of the video was used to calibrate the software so that measurements could be taken from the images if required. Selected frames saved in bitmap format were cropped and post processed by adjusting brightness and contrast levels. The actual height of the cropped schlieren video images is 42.6mm and the normal video images 27.5 mm.

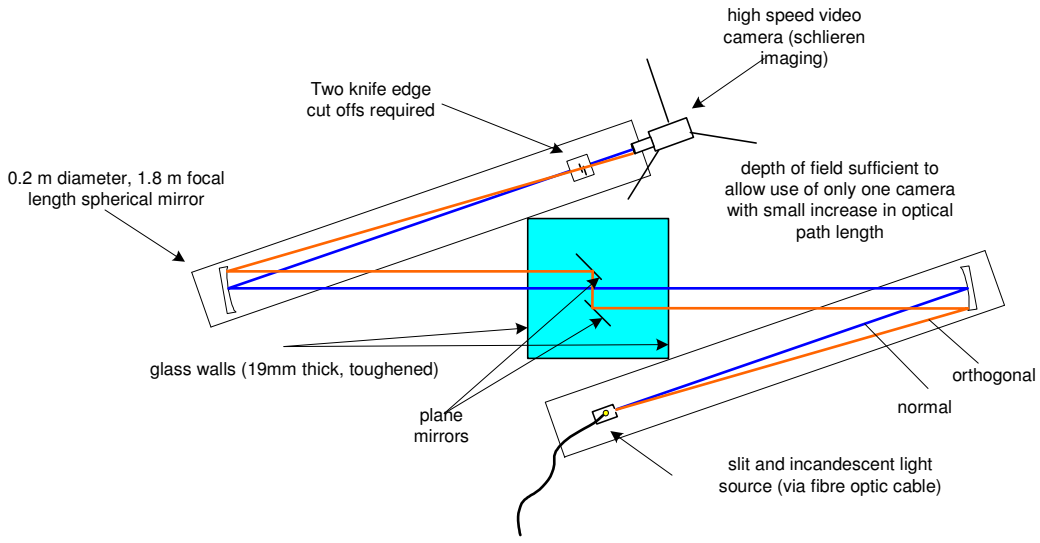

Figure 4. Schematic diagram of orthogonal schlieren system

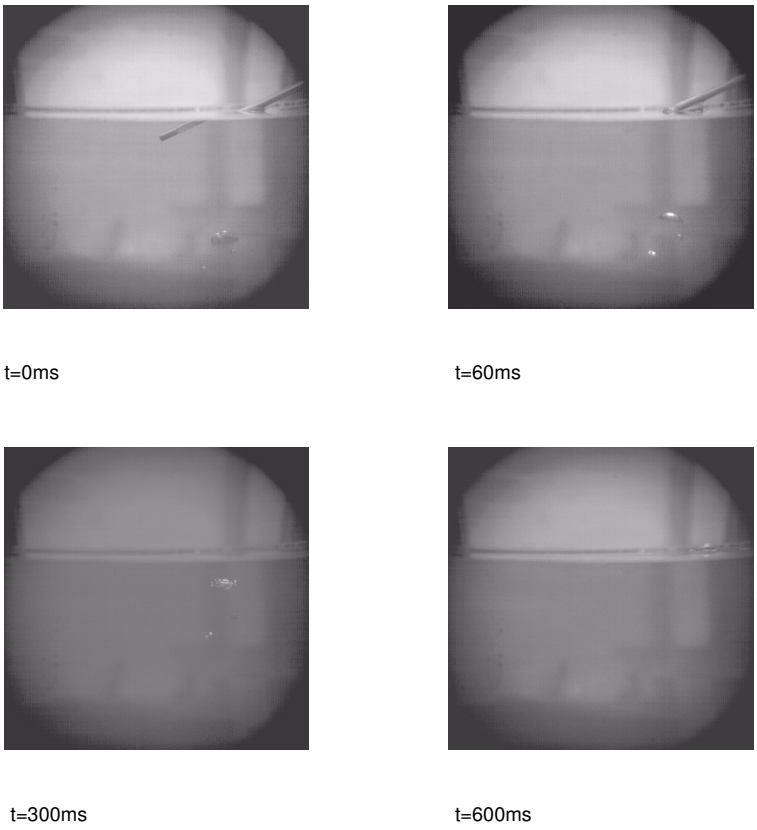

Figure 5. A sequence of still photographs taken from a digital video of a hydrogen bubble rising to a water surface

3.0 RESULTS

3.1 Bubble release and dispersion

Selected frames from the normal and schlieren imaging for the release of a typical bubble of 2.0 cm^3 volume are given in Figures 5 and 6. For convenience, the first frame selected from the normal video has been assigned t = 0 ms. Over the next two images the bubble (along with a much smaller bubble can be seen rising towards the surface of the water). It can be seen that the larger of the bubbles is significantly non-spherical. The last image shows the bubble formed on the water surface. It was observed that bubbles tend not to burst on arrival at the surface but are initially stable and persist for several tens of milliseconds. The first frame of the schlieren imaging sequence in Figure 6 shows the formation of a small wave on the water surface immediately preceding the emergence of the bubble. After 116 ms a bubble forms on the water surface. This persists for another 60 ms at which point the bubble bursts. The bubble then rapidly collapses over a few milliseconds. The hydrogen can be seen emerging from the bubble as a jet when it bursts, which then travels away from the site of the bubble. After 350 ms following the bubble burst, the jet/plume can still just be seen and extends around 110 mm from the bubble site. It was possible from the schlieren videos to estimate the extent and the duration of the hydrogen cloud formed by the bursting bubble.

The distance from the epicentre of the bursting bubble to the point at which the movement of hydrogen could no longer be seen on the non-enhanced images was defined as the visible detection limit. In general, it was observed that this limit increases with the bubble size. This can be seen clearly from the plot given in Figure 7.

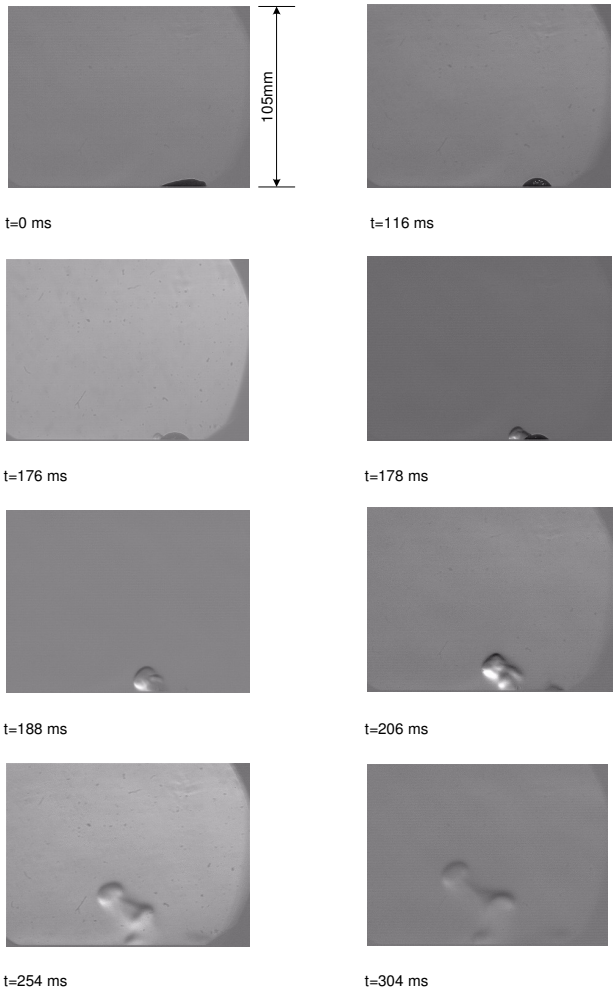

Figure 6. A sequence of schlieren images of an hydrogen bubble breaking a water surface and subsequently dispersing in air.

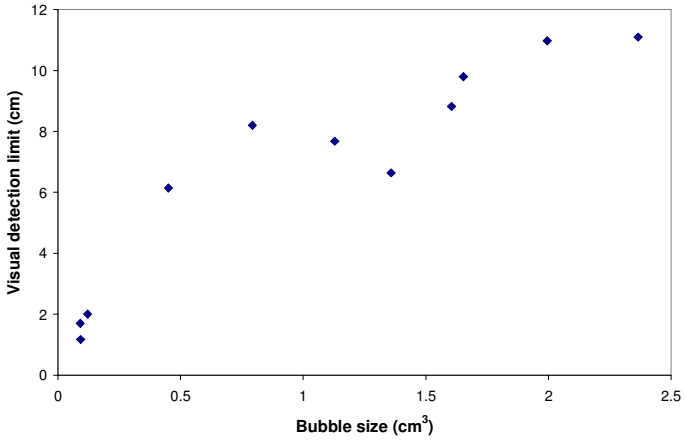

Figure 7. Visible detection limit vs bubble size

To examine bubble bursting behaviour in more detail the modified technique described in 2.3 was employed. An image sequence clearly showing the bursting mechanism of a 1.5 cm^3 bubble is given in Figure 8 where, frame 0 is the last frame prior to the initial appearance of a hole on the bubble surface. After 0.67 ms the hole can clearly be seen on the back surface of the bubble. The hole grows rapidly in size and by 2ms can be seen to extend almost from the waterline to the apex on the rear side of the bubble. It is interesting to note that during this period the bubble itself has not really altered in size. Frame 16 (2.67 ms) is the first where there is any appreciable change in the overall bubble size. Frame 16 is also the first frame where there are the very first signs of the rim of the hole starting to shed ligaments of water. These ligaments can be more clearly seen on Frame 28 (4.67 ms), by which time the bubble itself is almost completely gone with only a small part of the surface of the initial bubble remaining. By Frame 32 (5.33ms) the bubble has completely burst, although some ligaments of water and droplets shed from the rim remain in the air.

A schlieren video sequence of bursting of a 1.5 cm^3 bubble is shown in Figure 9. Frame 1 on the schlieren video extract appears to show an intact bubble, in fact there is actually a very small reduction in bubble size from Frame 0 indicating some loss of hydrogen. A tear starts close to the waterline on the rear surface of the bubble. By Frame 2 of the schlieren sequence, hydrogen can be seen just emerging from behind the left edge of the bubble. The formation of a rim which then sheds ligaments of water corresponds to Frame 4 of the schlieren video sequence. This frame clearly shows the almost fully collapsed bubble surrounded by cloud of hydrogen.

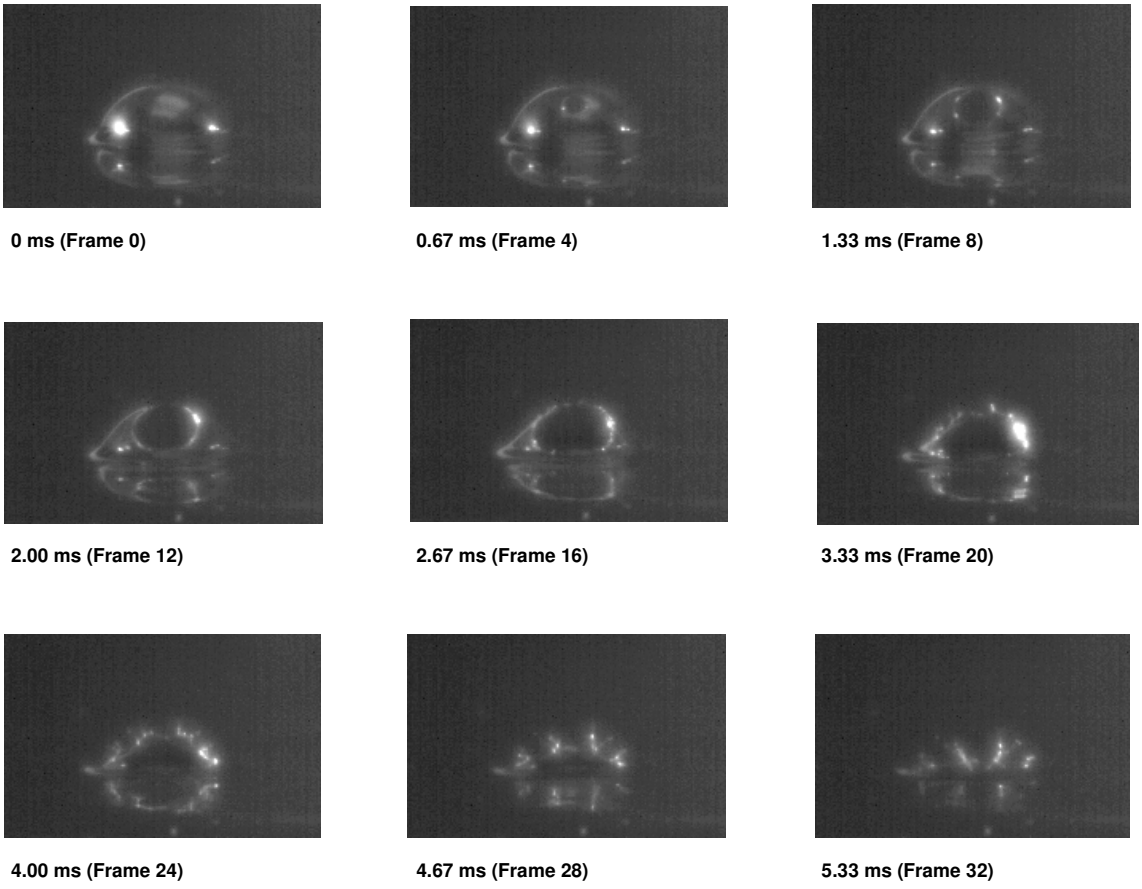

Figure 8. Video of 1.5 cm^3 bubble burst showing detail of bursting behaviour.

After a further few milliseconds the bubble has gone and a few splashes/droplets of water can be seen being thrown outwards. The bubble burst clearly happens very much faster than the dispersion,

although some hydrogen is clearly forced from the bubble as it bursts much appears to essentially remain in place as the bubble film peels/tears away. This can be seen on Frame 4 of the schlieren video, the hydrogen occupying only slightly more volume than the original bubble. Following the bubble burst the hydrogen can be seen to disperse outwards and upwards, appearing to detach from the surface after about 60 ms.

Table 1. Summary of bubble burst data

Bubble size. cm^3	Burst Time. ms	Nucleation position	Plume dispersion. mm
1.5	5.8	High	
1.5	6.0	Waterline	34
1.4	4.7	Mid	29
1.3	3.5	High	34
1.2	4.7	Low	54
1.1	5.8	Low	
1.0	2.7	Top	
0.9	5.7	Waterline	46
0.2	2.2	High	

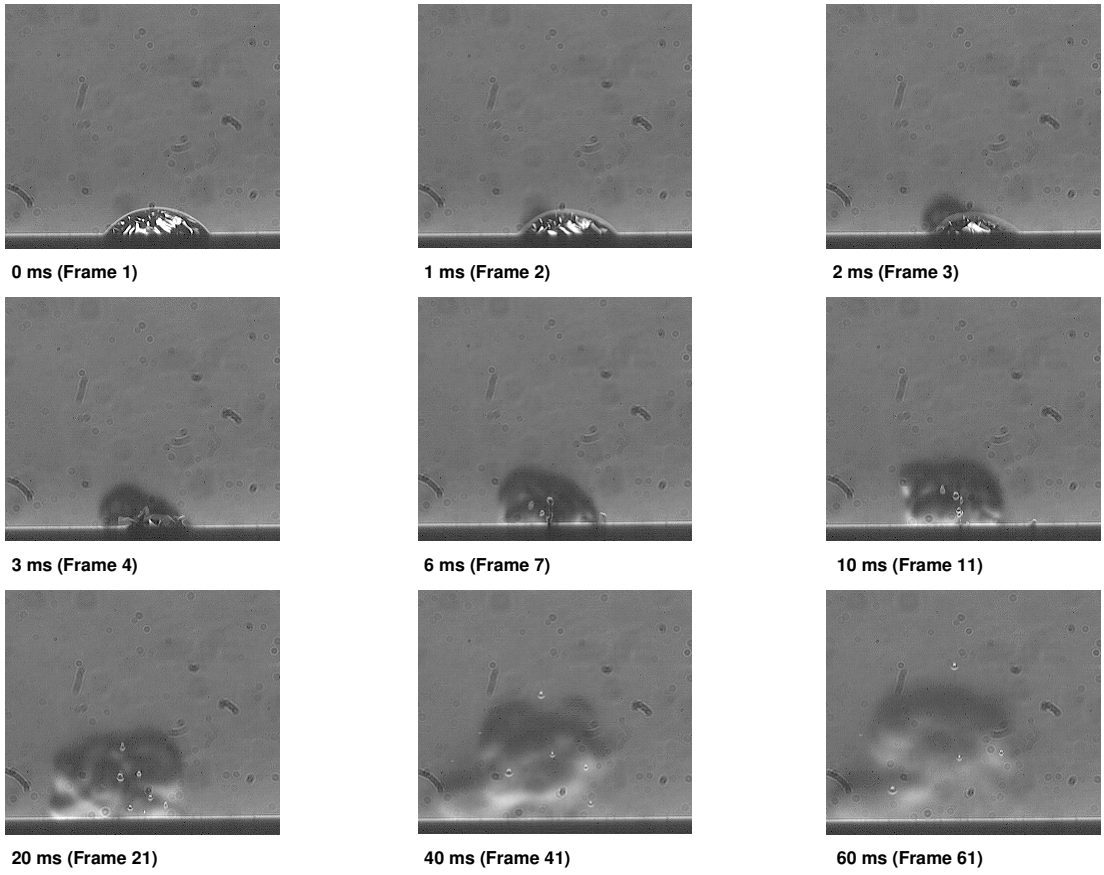

Figure 9. Schlieren image sequence of a 1.5 cm^3 hydrogen bubble burst and dispersion.

From the experimental test results it was found that there was significant variation in both bubble burst times, hole nucleation and the height to which the plume was dispersed above the water surface (after 60 ms). This is summarised in Table 1.

3.2 Visible schliere flammability test results

Hydrogen containing clouds that clearly did not appear to touch the igniter were found not to ignite. Consequently they were ignored with regard to ignition frequency since no useful information could be inferred from their non-ignition. Considering only the clouds producing schliere that did appear to touch the igniter on both orthogonal images, it was clear that the movement of the schliere does accurately pinpoint the region of enhanced hydrogen concentration.

The results obtained with the igniter positioned at three different heights above the water surface, are given in Table 2.

Table 2. Ignition frequency

Igniter Height, mm	Ignition Frequency
40	22/31
53	6/30
65	0/27

It can be seen that there is a quite rapid drop in ignition probability with distance from the bubble burst. From the work reported in section 2 it was determined that, for the size of bubbles in question, plumes would remain visible for around 100 mm from the site of release. Clearly therefore plumes are becoming non-ignitable (i.e. by the test igniter) well within this distance.

4.0 DISCUSSION

An apparatus has been built for studying dispersion of hydrogen releases from beneath a liquid surface. It utilises a high speed digital imaging system to film bubble rise through the liquid to the surface and a high speed Z-type schlieren video system for visualising the hydrogen release on bubble burst and the subsequent dispersion process. Two sets of experiments were conducted, bubble dispersion experiments to indicate the mechanism involved and an additional set of experiments to relate schliere intensity to flammability.These latter experiments are of importance since the analysis of grey scale schlieren images cannot directly yield hydrogen concentration data. However, hydrogen concentrations down to about 4% (v/v) can be seen using the schlieren technique which detects refractive index gradients in the plane normal to the optical axis. The strongest refractions occur at the points where the concentration gradient is greatest, rather than where the concentration of hydrogen is highest. The experiments relating schliere intensity to flammability were essentially carried out to ascertain whether a bursting hydrogen bubble could be ignited if the schliere from the bubble had become undetectable.

The igniter used in this work was capable of igniting hydrogen in air mixtures down to 6.25% v/v (around the limit for sideways flame propagation) and it was shown using the orthogonal schlieren system that when the igniter is placed slightly inside the visible detection range, the hydrogen cannot be seen to ignite. The implication is that the visible detection limit determined with the schlieren system can be used to decide whether or not hydrogen from a bubble will ignite at a given distance from the epicentre of the bursting bubble. From Table 2 it can be seen that there is a quite rapid drop in ignition probability with distance from the bubble burst. It was also determined that, for the size of bubbles in question, plumes would remain visible for around 100mm from the site of release. Clearly therefore plumes are becoming non-ignitable by the igniter well within this distance.

At a distance greater than the visible detection limit, bubbles up to 2.5 cm^3 do not ignite. At distances less than the visible detection limit, ignition of the hydrogen from such bubbles must be regarded as credible, albeit not absolutely certain.

Considering the results of the bubble dispersion experiments, there is a transition from spherical to approximately cap shape of the rising bubbles at relatively small bubble volumes ~ 0.3 cm^3 and that bubbles generally persist on the water surface for significant time periods before bursting. From the high speed video sequences it is possible to describe a physical mechanism for the hydrogen bubble burst. Following the nucleation of a hole, surface tension causes the film to peel back rapidly forming a ring/torus of water around the enlarging hole. The rapid retraction of the film, occurring in only a few milliseconds, then induces rim instability resulting in the formation of ligaments extending normal to the bubble surface as a result of the centripetal acceleration. Similar behaviour has been reported in the literature [2]; the velocity of the retracting rim, derived from balancing the retraction force due to surface tension with the inertia of the growing rim is given for a film of uniform thickness (h) by $V = (2\sigma/\rho\ h)^{1/2}$ where σ is the surface tension and ρ the water density.

It is clear from the results summarised in Table 1 that there is significant variation in both bubble burst times, hole nucleation site and the height to which the plume has dispersed above the liquid surface (after 60ms). Some of the results can be readily explained, for example the relatively short burst time for a bubble bursting near its top is perhaps not unexpected as it coincides with the least distance from nucleation site to waterline for complete disappearance of the bubble film i.e the rim needs to travel a maximum of only ¼ of the bubble circumference as opposed to half for a waterline burst. It is also not surprising that the very small 0.2 cm^3 bubble was the fastest bursting.

5. CONCLUSIONS

An experimental study to specifically investigate the bursting of hydrogen filled water bubbles and the influence of the bursting process on dispersion has been carried out. This has furthered understanding of the behaviour of hydrogen bubbles rising through water, bursting and their subsequent dispersion. It has also been shown that the visible extinction limit with schlieren imaging approximates to concentrations of hydrogen approaching the lower flammable limit of hydrogen in air.

The release of hydrogen filled water bubbles from 0.2 to 1.5 cm^3 has been examined using normal and schlieren high speed video. For the bubbles investigated, bursting was found to occur over a period of a few ms. The bubble films peel back from an initial hole, due to surface tension, forming a rim of water around the edge of the hole as it enlarges. The rim itself then becomes unstable and begins to form ligaments shedding small water droplets. The water film essentially peels away over the surface of the hydrogen leaving a hemisphere of hydrogen gas, although some hydrogen can be seen being forced out as bursting/collapse occurs. There was significant variation in the burst times and the extent to which hydrogen initially dispersed, due to random variations in the bubble bursting process.

Acknowledgments

The Hydrogen Hazards Unit (HHU) at London South Bank University would like to acknowledge the financial support of Sellafield Ltd and the University in undertaking this and similar programmes of work on ignitions caused by mechanical stimuli. Thanks are also due to S. Jones for his help and the technical support given in the LSBU Engineering Workshops.

References

1. Settles G.S., Schlieren and shadowgraph techniques; Visualizing phenomena in transparent media., Springer, Berlin, 2001.
2. Lhuissier H. and Villermaux E., Bursting Bubbles, *Physics of Fluids*, 21, Sept., 2009, 091111(1)